JACS
JOURNAL OF THE AMERICAN CHEMICAL SOCIETY

Article

pubs.acs.org/JACS

Chemical Modification of a Dehydratase Enzyme Involved in Bacterial Virulence by an Ammonium Derivative: Evidence of its Active Site Covalent Adduct

Concepción González-Bello,*[,§] Lorena Tizón,[§] Emilio Lence,[§] José M. Otero,[†] Mark J. van Raaij,[∥] Marta Martinez-Guitian,[⊥] Alejandro Beceiro,[⊥] Paul Thompson,[‡] and Alastair R. Hawkins[‡]

[§]Centro Singular de Investigación en Química Biológica y Materiales Moleculares (CIQUS) and [†]Departamento de Bioquímica y Biología Molecular and CIQUS, Universidad de Santiago de Compostela, 15782 Santiago de Compostela, Spain

[∥]Departamento de Estructura de Macromoléculas, Centro Nacional de Biotecnología (CSIC), Campus Cantoblanco, 28049 Madrid, Spain

[⊥]Servicio de Microbiología-INIBIC, Complejo Hospitalario Universitario A Coruña (CHUAC), 15006 A Coruña, Spain

[‡]Institute of Cell and Molecular Biosciences, Medical School, University of Newcastle upon Tyne, Newcastle upon Tyne NE2 4HH, United Kingdom

Supporting Information

ABSTRACT: The first example of an ammonium derivative that causes a specific modification of the active site of type I dehydroquinase (DHQ1), a dehydratase enzyme that is a promising target for antivirulence drug discovery, is described. The resolution at 1.35 Å of the crystal structure of DHQ1 from *Salmonella typhi* chemically modified by this ammonium derivative revealed that the ligand is covalently attached to the essential Lys170 through the formation of an amine. The detection by mass spectroscopy of the reaction intermediates, in conjunction with the results of molecular dynamics simulations, allowed us to explain the inhibition mechanism and the experimentally observed differences between *S. typhi* and *Staphylococcus aureus* enzymes. The results presented here reveal that the replacement of Phe225 in *St*-DHQ1 by Tyr214 in *Sa*-DHQ1 and its hydrogen bonding interaction with the conserved water molecule observed in several crystal structures protects the amino adduct against further dehydration/aromatization reactions. In contrast, for the *St*-DHQ1 enzyme, the carboxylate group of Asp114, with the assistance of this water molecule, would trigger the formation of a Schiff base that can undergo further dehydration reactions until full aromatization of the cyclohexane ring is achieved. Moreover, *in vitro* antivirulence studies showed that the reported compound is able to reduce the ability of *Salmonella* Enteritidis to kill A459 respiratory cells. These studies have identified a good scaffold for the design of irreversible inhibitors that can be used as drugs and has opened up new opportunities for the development of novel antivirulence agents by targeting the DHQ1 enzyme.

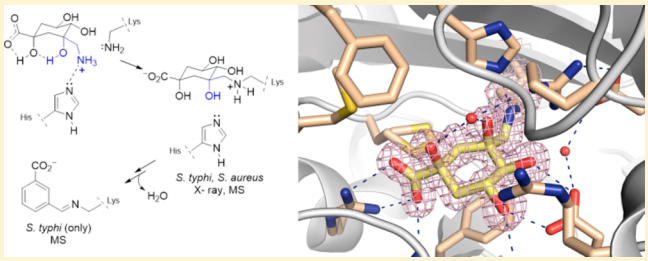

INTRODUCTION

The increasing and widespread development of resistance to antibiotics has made infectious diseases one of the most important public health issues in both community and clinical settings.[1] The World Health Organization currently considers antibiotic resistance to be one of the three greatest threats to human health in the coming decades. Hence, there is great interest in the development of alternative therapies, the identification of unexplored bacterial targets, and the discovery of new strategies for the treatment of infections that are resistant to current antibiotics.[2] The most widely used strategy to combat bacterial infections is based on the disruption of their viability by preventing the synthesis and assembly of key components for bacterial survival, such as cell wall biosynthesis, DNA replication, RNA transcription, folate biosynthesis, and protein biosynthesis.[3] Although this strategy is highly effective and many antibiotics in clinical use are based on this principle, it causes substantial stress to the bacterium, and this favors the growing emergence of antibiotic-resistant strains. To avoid this issue, in recent years a great deal of effort has been devoted to the development of alternative approaches. Targeting bacterial virulence or disrupting the interaction between the host and the pathogen is an attractive choice that is increasingly being explored.[2,4] Antivirulence drugs will create an *in vivo* scenario similar to that achieved by vaccination with a live attenuated strain. In this context, it has been suggested that the type I dehydroquinase enzyme (DHQ1, 3-dehydroquinate dehydratase, EC 4.2.1.10), the third enzyme in the biosynthesis of aromatic amino acids, may act as a virulence factor *in vivo* as the

Received: April 20, 2015
Published: July 6, 2015

DOI: 10.1021/jacs.5b04080
J. Am. Chem. Soc. 2015, 137, 9333−9343

deletion of the *aro*D gene, which encodes DHQ1 from *Salmonella typhi* and *Shigella flexneri*, has been proven to afford satisfactory live oral vaccines, with the latter providing monkeys with protection against oral challenge with live *S. flexneri* 2457T.[5] This finding, together with the fact that DHQ1 does not have any counterpart in human cells, has pinpointed DHQ1 as a promising target in the search for new antivirulence agents to combat widespread antibiotic resistance. Hence, there is great interest in developing efficient inhibitors of this enzyme as well as obtaining a detailed knowledge of its mechanism of action for the rational design of inhibitors that can be used as drugs.

DHQ1 is present in plants and several pathogenic bacteria, such as *Escherichia coli*, *S. typhi*, and *Staphylococcus aureus*. DHQ1 is a class I aldolase enzyme that catalyzes the reversible *syn* elimination of water in 3-dehydroquinic acid (**1**) to form 3-dehydroshikimic acid (**2**) by a multistep mechanism that involves the formation of Schiff base species (Scheme 1).[6] The

Scheme 1[a]

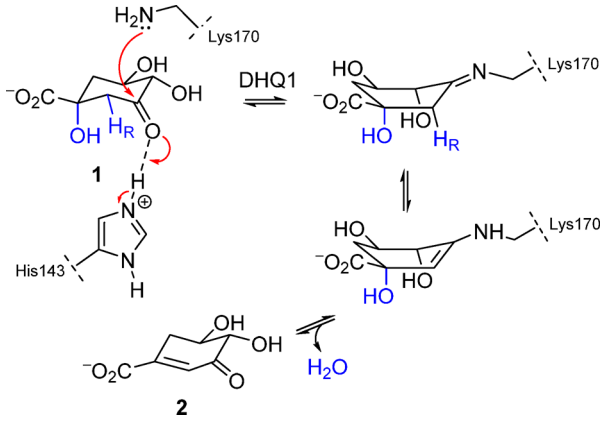

[a]Enzymatic conversion of 3-dehydroquinic acid (**1**) to 3-dehydroshikimic acid (**2**) catalyzed by DHQ1.

reaction is initiated by the formation of the substrate-Schiff base between the C3 carbonyl group of the substrate and an essential lysine (Lys170 in *S. typhi*). Once the substrate-Schiff base has been formed, a base residue of the active site removes the pro-*R* hydrogen at C2 in **1** to afford an enamine, which undergoes acid-catalyzed elimination of the C1 hydroxyl group, a reaction that is mediated by a histidine (His143 in *S. typhi*) acting as a proton donor. It has been suggested that the formation of the substrate-Schiff base involves a distortion of the cyclohexane ring to align the bond of the pro-*R* hydrogen at C2 (pseudoaxial) with the π-orbital of the imine that increases its acidity.[6c,e,f] The role in the enzymatic mechanism of this histidine has been the subject of much controversy. Based on the proximity of His143 to the C2 carbon in the crystal of the substrate-Schiff base, this essential residue was highlighted as the base that removes the pro-*R* hydrogen at C2.[7] However, its role as a general base appears to be more complex because the H143A variant protein is able to slowly transform substrate to product and stalls the hydrolytic release of product from the active site.[8] It seems clear that His143 is involved in both the formation and subsequent hydrolysis of the Schiff base intermediates.

It is important to highlight that this enzymatic reaction is also catalyzed by the type II dehydroquinase enzyme (DHQ2), but by entirely different mechanism and stereochemical courses.[9,10] In contrast to DHQ1: (a) no covalent attachment of the substrate to the enzyme through Schiff base formation is involved; (b) the loss of the more acidic pro-*S* hydrogen from C2 in **1** via the formation of an enolate intermediate takes place;[11] (c) compounds targeting the DHQ2 enzyme would have an influence on bacterial viability (antibiotics) rather than bacterial virulence. Considering that DHQ2 is essential in *Mycobacterium tuberculosis* (*aroD* gene) and *Helicobacter pylori* (*aroD*/*aroQ* gene), many inhibitors of the DHQ2 enzyme for the development of novel antitubercular antibiotics as well as new drugs for the treatment of infectious diseases caused by *H. pylori* have been described.[12] Those compounds are either analogs of the natural substrate[13] or mimetics of the enolate intermediate[14] having in both cases inhibition potencies in the nanomolar range. An ester prodrug approach of those inhibitors proved to increase permeability into the mycobacterial cell and optimal *in vitro* activities were obtained.[14] More recently, in the search for drug-like inhibitors, several 3-nitrobenzylgallate-based analogs have also been described.[15] However, these aromatic derivatives proved to have considerably lower inhibitory potencies (micromolar range) probably due to less efficient binding interactions with the carboxylate binding pocket that seems to be relevant for good binding affinity.

To date, very few irreversible inhibitors of DHQ1 have been reported (Figure 1).[17,18] Most of these incorporate reactive

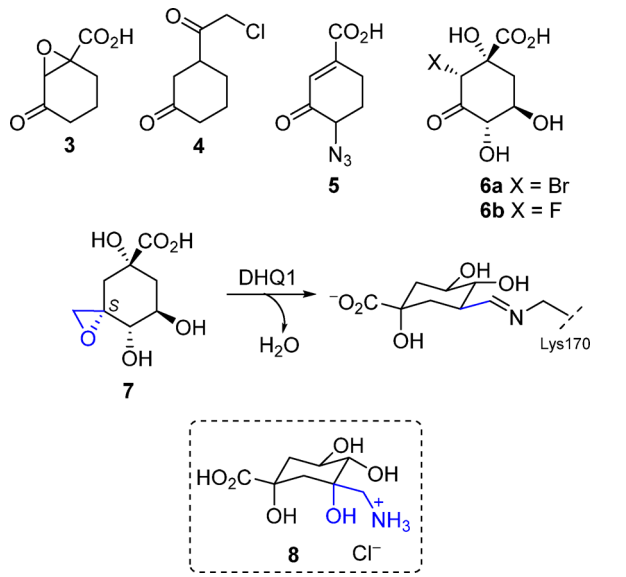

Figure 1. Irreversible inhibitors of DHQ1, compounds **3**–**7**, chemical modification of *St*-DHQ1 by **7**, and target compound **8**.

electrophilic functional groups and have been described as racemic mixtures. Among them, we have recently shown that chiral epoxide **7**, which is a mimetic of the natural substrate with an *S* configuration at C3, causes the chemical modification of the enzyme.[17c] The resolution of the crystal structure of DHQ1 from Salmonella typhi (*St*-DHQ1) covalently modified by *S* epoxide **7** revealed the formation after several chemical modifications of a stable Schiff base with the essential Lys170. Biochemical and computational studies on this compound and its epimer, an epoxide with the *R* configuration at C3, provided strong evidence that the enzyme appears to be designed to form the substrate-Schiff base by activation and correct positioning of the oxygen atom of the ketone group in **1** by

DOI: 10.1021/jacs.5b04080
J. Am. Chem. Soc. 2015, 137, 9333–9343

His143 and subsequent nucleophilic attack by Lys170 from the Si face of the ketone group.

Based on these initial results, and in the search for irreversible inhibitors that do not bear such reactive functional groups for use as drugs, we report herein a mimetic of the natural substrate, namely ammonium derivative **8**, which is an irreversible inhibitor of DHQ1 from *S. typhi* and *S. aureus* (*Sa*-DHQ1). The resolution at 1.35 Å of the crystal structure of *St*-DHQ1 chemically modified by ammonium derivative **8** revealed that the ligand is covalently attached to the essential Lys170 by the formation of an amine. The detection by mass spectroscopy of the reaction intermediates, as well as the results of docking and molecular dynamics (MD) simulation studies, allowed us to explain the experimentally observed differences between the two enzymes and to understand the inhibition mechanism. Moreover, the *in vitro* efficacy of compound **8** to inhibit bacterial virulence was also studied. To our knowledge, this is the first example of an ammonium derivative that causes the specific modification of the active site of a dehydratase enzyme and that it is also a promising target for antivirulence drug discovery.

RESULTS AND DISCUSSION

Synthesis of Ammonium Derivative 8. The target compound was prepared from previously reported epoxide **9**[17c] (Scheme 2). Nucleophilic ring opening of epoxide **9** by

Scheme 2[a]

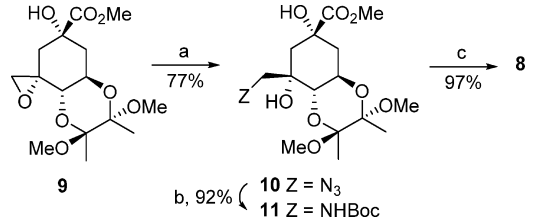

[a]Reagents and conditions: (a) NaN_3, *p*-$NO_2C_6H_4CO_2H$, 15-crown-5, DMF, 115 °C; (b) (i) H_2, Pd/C (10%), MeOH, RT, (ii) Boc_2O, Et_3N, DMF, RT; (c) HCl (0.3 M), 100 °C.

treatment with sodium azide in the presence of catalytic amounts of 15-crown-5 ether and *p*-nitrobenzoic acid afforded azide **10** in 77% yield. The presence of this acid was key for the reaction to proceed. Organic acids with lower pK_a values, such as benzoic acid, led to lower conversion and lower yields. Azide **10** was reduced to the amine by catalytic hydrogenolysis with palladium on carbon as the catalyst. Purification of the resulting free amine was difficult, and consequently, the crude amine was protected with di-*tert*-butyl dicarbonate to give Boc-amino-protected **11**. Finally, hydrolysis of methyl ester **11** with concomitant removal of the protecting groups gave an excellent yield of amino alcohol **8** as the hydrochloride salt.

Inhibitory Activity of 8. Ammonium derivative **8** was found to be a time-dependent irreversible inhibitor of the two enzymes (Figure 2). The inactivation proved to be more efficient for *Sa*-DHQ1 than for *St*-DHQ1. Thus, a 210 μM concentration of **8** caused ~60% inactivation of *Sa*-DHQ1 vs ~20% of *St*-DHQ1 after ~30 min. A level of ~60% inactivation of *Sa*-DHQ1 was also obtained with lower concentrations of **8** (84 μM) after incubation for 3 h. Higher concentrations of **8** (840 μM) provided a barely detectable enzymatic activity of *Sa*-DHQ1 after approximately 15 min. The K_i and k_{inact} values of

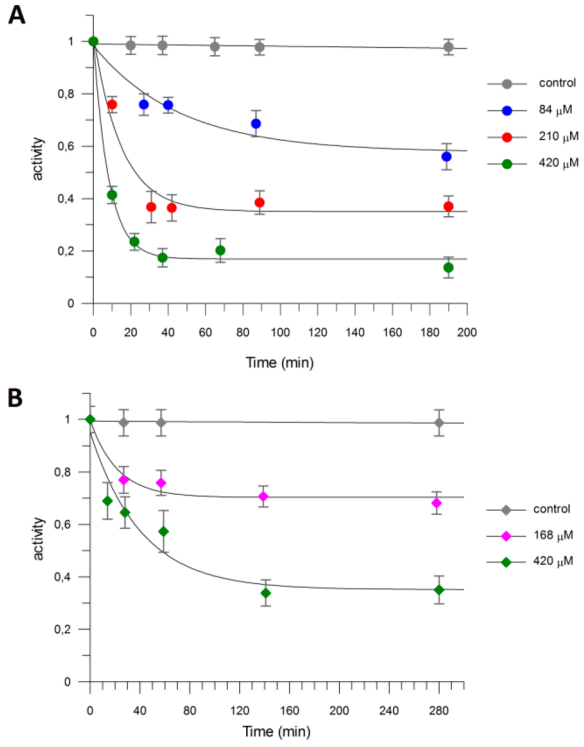

Figure 2. Variation of the enzymatic activity of DHQ1 with time without incubation and after incubation with increasing amounts of ammonium derivative **8**: (A) *Sa*-DHQ1 and (B) *St*-DHQ1. Error bars represent standard deviation calculated for three independent experiments. Assay conditions were PPB (50 mM, pH 7.2) at 25 °C.

compound **8** against the two enzymes were obtained from Kitz–Wilson plots (Figure S1). Ammonium derivative **8** showed K_i values of 905 ± 10 and 934 ± 40 μM and k_{inact} values of 5.3 ± 0.1 and 3.4 ± 0.1 ms^{-1} against *Sa*-DHQ1 and *St*-DHQ1, respectively. Under the assay conditions, the kinetic parameters for *St*-DHQ1 and *Sa*-DHQ1 were K_m = 18 ± 3 μM; k_{cat} = 255 ± 12 s^{-1}, and K_m = 24 ± 3 μM; k_{cat} = 1.1 ± 0.1 s^{-1}, respectively.

Detection of Chemical Modifications. The possible chemical modification of samples of inactivated enzymes was also studied by mass spectrometry (matrix-assisted laser desorption ionization, MALDI). Significant differences were found in the mass spectra of samples of DHQ1 enzymes inactivated by **8** (Figures 3 and S2). The mass spectrum of the

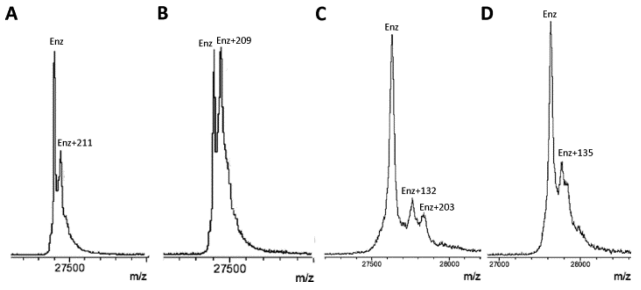

Figure 3. MALDI spectra of samples of DHQ1 chemically modified by **8**. (A) *Sa*-DHQ1 chemically modified by **8** (420 μM). (B) *Sa*-DHQ1 chemically modified by **8** (840 μM). (C) *St*-DHQ1 chemically modified by **8** (420 μM). (D) *St*-DHQ1 chemically modified by **8** (420 μM) and subsequent treatment with sodium borohydride. Assay conditions were PPB (50 mM, pH 7.2) at 25 °C.

DOI: 10.1021/jacs.5b04080
J. Am. Chem. Soc. 2015, 137, 9333–9343

Sa-DHQ1 enzyme consisted of a peak for the unmodified protein (calculated mass 27,003) and a second peak for a covalently modified protein, corresponding to an additional mass of 209 or 211 on separate samples (Figure 3A,B). For *St*-DHQ1, in addition to the unmodified protein (calculated mass 27,655) and the peak for the covalently modified protein corresponding to an additional mass of 203, a third peak corresponding to an additional mass of 132 was identified (Figure 3C).

These results suggest that in both cases the nucleophilic substitution of the amino group had taken place (expected mass increase of 203). However, further chemical modifications are likely to occur for the *St*-DHQ1 enzyme. Reasoning that the peak corresponding to an additional mass of 132 could be due to subsequent dehydration of the initial adduct triggered by the formation of a Schiff base as for epoxide **7**, samples first incubated with ammonium derivative **8** for 1 h were subsequently treated with sodium borohydride and analyzed by MALDI. The resulting mass spectrum corroborated this hypothesis, and the corresponding reduced form of the chemically modified *St*-DHQ1 enzyme was observed (Figure 3D). It is important to highlight that significant differences were not observed for inactivated *Sa*-DHQ1 samples treated with sodium borohydride. In an effort to gain a further insight into the inhibition mechanism of ammonium derivative **8** and to understand the experimentally observed differences between the *S. aureus* and *S. typhi* enzymes, structural and MD simulation studies were carried out. The results of these studies are discussed below.

X-ray Crystal Structure of the *St*-DHQ1/8 Adduct. The crystal structure of *St*-DHQ1 covalently modified by its inhibitor **8** was obtained by soaking apo-*St*-DHQ1 crystals, and the structure was solved at 1.35 Å (Figure 4). Crystals were mounted into cryoloops and were directly flash frozen by rapid immersion in liquid nitrogen. X-ray diffraction data were collected from crystals cryo-cooled in a stream of cold nitrogen gas (100 K) at ambient pressure using synchrotron radiation, and the data were subsequently processed. The structure was determined by molecular replacement, using the previously described structure of the reduced form of the *St*-DHQ1 product-Schiff base intermediate (PDB entry 1QFE),[8c] as a search model and the structure was refined. A summary of the statistical data following data reduction and processing is given in Table 1.

Unbiased, calculated electron density maps showed clear electron density for the enzyme-modified inhibitor molecule **8** (Figure 4A). The reported crystal structure shows that the ligand is covalently attached to Lys170 by an amine, and the substrate-covering loop is in the closed conformation. In contrast to the previously reported *St*-DHQ1/**7** adduct (PDB entry 4CLM),[17c] dehydration of the C3 hydroxyl group did not take place, as clear electron density was observed for this hydroxyl group (Figure S3). It is worth highlighting that this structure was obtained by soaking, whereas the previous one was obtained by cocrystallization after several weeks. In addition, the Lys170 side chain is now ordered, and the C3 hydroxyl group establishes a strong hydrogen bonding interaction with a water molecule (W134) that is found in several crystal structures forming a bridge between Arg82 and the C1 hydroxyl group. As in PDB entry 4CLM and in the Michaelis complex,[17c] the modified ligand **8** binds to the active site by a salt-bridge between its carboxylate group and the guanidinium group of the conserved Arg213, which has

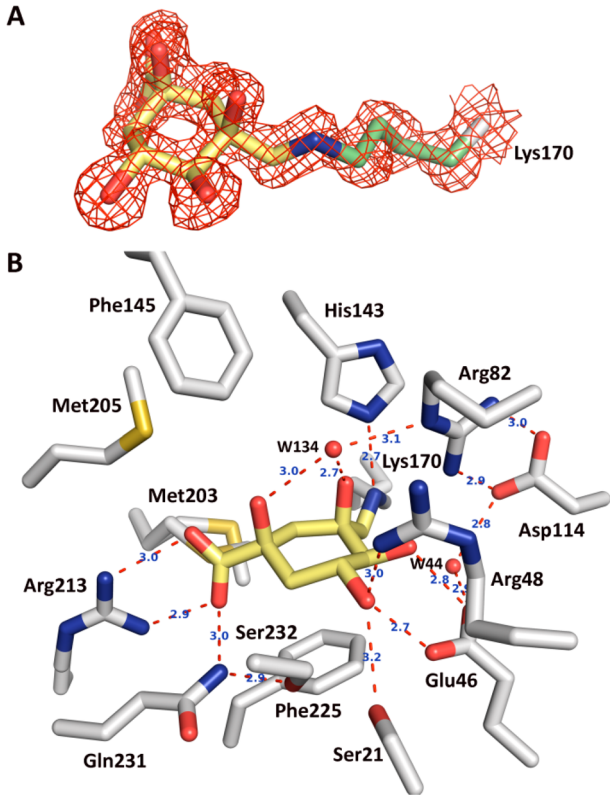

Figure 4. Crystal structure of *St*-DHQ1 covalently modified by ammonium derivative **8**. (A) Unbiased electron density for the modified inhibitor **8** (yellow) and its covalent attachment to Lys170 of *St*-DHQ1 (green). From the model obtained by molecular replacement and before inclusion of the inhibitor molecule, refinement was performed to obtain unbiased density for the inhibitor molecule and other model changes. A maximum-likelihood weighted $2F_o - F_c$ map contoured at 1σ is shown up to 1.6 Å around the inhibitor molecule and Lys side chain (red). The final model, including the inhibitor molecule, is superimposed onto the map. (B) Interactions of the modified inhibitor **8** with *St*-DHQ1 (gray). Hydrogen-bonding and electrostatic interactions (red) between the ligand and *St*-DHQ1 are shown. Relevant residues are shown and labeled.

previously been identified by chemical modification as the key residue for carboxylate recognition[10] and by a bidentate hydrogen bond between the carboxylate group of the conserved Glu46 and the C4 and C5 hydroxyl groups of the ligand (Figure 4B). The ligand is also anchored to the active site by several strong hydrogen-bonding interactions, which include two residues that are located in the substrate-covering loop, Gln231 and Ser232, Arg48, His143 and Ser21, and with Arg82 and Asp114 via two water molecules (W134 and W44, respectively). Moreover, the cyclohexane ring of the ligand is located on top of the Phe225 through the formation of key CH−π interactions. This residue, which is embedded into an apolar pocket involving Ile201, Val139, Leu78, and Ala223, seems to act as a "bottom lid" of the active site to isolate this part of the active site from the solvent environment, and it also blocks one of the faces of the substrate for catalysis.

MD simulation studies were conducted in order to obtain further details on the binding mode of the ligand in the *St*-DHQ1/**8** adduct and to gain an insight into the differences observed between the two enzymes. Considering that the covalent attachment of the reaction product molecule (as reduced from) to the DHQ1 from *Escherichia coli* causes a

DOI: 10.1021/jacs.5b04080
J. Am. Chem. Soc. 2015, 137, 9333−9343

Table 1. Crystallographic Data Collection and Refinement Statistics for the *St*-DHQ1/8 Adduct[a]

	St-DHQ1/**8**
Data Processing[a]	
space group	*I*2
cell parameters (*a*, *b*, *c*, *β*), Å, °	a = 67.40, b = 42.33, c = 84.83, *β* = 105.13
wavelength (Å)	0.97996
detector	ADSC Q315r CCD
observed reflections[b]	182,812 (26,519)[c]
resolution range (Å)	45.48−1.35 (1.42−1.35)
Wilson B (Å^2)	8.0
multiplicity	3.6 (3.6)
completeness	0.993 (0.993)
R_{merge}	0.068 (0.395)
Refinement[d]	
resolution range (Å)	37.63−1.35 (1.42−1.35)
reflections used in refinement[c]	48,464 (7025)
reflections used for R_{free}	2060 (315)
R factor[e]	0.174 (0.197)
R_{free}[f]	0.214 (0.264)
rmsd [bonds (Å)/angles (°)]	0.010/1.5
Final Model	
protein/inhibitor/water/sodium/chloride atoms	1966/14/199/2/2
average B protein/inhibitor/water/sodium/chloride (Å^2)	8.6/11.4/17.8/8.7/8.8
Ramachandran statistics[g] (%)	98.4/100.0
PDB accession code	4UIO

[a]Results from SCALA.[24] [b]No *σ* cutoff or other restrictions were used for inclusion of reflections. [c]Values in parentheses are for the highest resolution bin, where applicable. [d]Results from REFMAC.[30] [e]*R*-factor = $\sum||F_{obs}(hkl)| - |F_{calc}(hkl)||/\sum|F_{obs}(hkl)|$. [f]According to Brünger.[29] [g]According to the program MOLPROBITY.[31] The percentages indicated are for residues in favored and total allowed regions, respectively.

dramatic increase in the stability of the protein against proteolysis,[8c] a similar behavior would be expected for the reported chemical modified *St*-DHQ1 enzyme.

Covalent Modification Mechanism. First, the protonation state of the essential His143 and Lys170 in the reported crystal structure was studied. The monomer structure in aqueous solution using the molecular mechanics force field AMBER was employed. Four possibilities were considered, i.e., a dual (*δ* and *ε*) and a single (*δ*) protonation state of His143 and free and protonated forms of Lys170 (Figures 5 and S4). Analysis of the variation of the distances involving the NZ atom of Lys170 and the NE2 atom of His143, the OD2 atom of Asp114, and the oxygen atom of WAT44 during 50 ns of dynamic simulation and comparison with the reported crystal structure clearly showed that in the reported crystal structure His143 is protonated in the *δ* position and the Lys170 is in its protonated form. In this arrangement, the His143 side chain, the carboxylate group of Asp114, and W44 are in close contact with the NZ atom of Lys170.

Previously reported biochemical and computational studies on the substrate-Schiff base formation pinpointed His143 as the residue involved in the deprotonation of the initial adduct resulting from nucleophilic attack of the *ε*-amino group of Lys170 to the C3 ketone group of the natural substrate.[19] Similarly, covalent attachment of **8** would probably occur by nucleophilic attack of Lys170 with the release of ammonia and

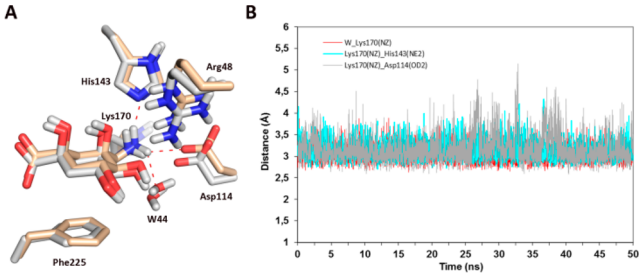

Figure 5. (A) Comparison of the binding mode of the ligand in the *St*-DHQ1/**8** adduct after minimization and prior to simulation (gray) and after 50 ns of dynamic simulation (light orange). The protonated forms of Lys170 and His143 (ND1) are considered. Relevant side chain residues are shown and labeled. (B) Variation of the distances involving the NZ atom of Lys170 and the NE2 atom of His143, the OD2 atom of Asp114, and the oxygen atom of W44 during the whole simulation. The protonated forms of Lys170 and His143 (*δ*) were considered.

by activation from the opposite site of the histidine acting as a Lewis acid (Figure 6D, path a). An analysis of enzymatic activity of DHQ1 after incubation with compound **8** at different pH values (5.8, 7.0, and 8.0) revealed that the enzyme inactivation is less efficient at high pH (Figure S11). This pH conditions would reduce the amount of protonated amino group in **8**, which is required as leaving group. Moreover, an intramolecular cyclization of **8** to afford epoxide **7**[17c] followed by epoxide opening by the *ε*-amino group of Lys170 might be considered (Figure 6D, path b). The spectroscopic monitoring of the possible formation of epoxide **7** from ammonium derivative **8** in solution at different pH conditions reveals that this process does not occur in the absence of enzyme (Figures S12 and S13). However, considering that DHQ1 active site is largely shielded from the solvent environment for catalysis,[20] the reactive side chain residues and ligands are likely to be desolvated and a high effective concentration of a nucleophile would be therefore achieved. It might be then also possible that the ammonium derivative **8** undergoes an intramolecular cyclization to give epoxide **7** in the active site. Both pathways would afford the experimentally observed adduct **12**.

The close proximity of the His143 side chain (Figure 5) and previous computational studies with the natural substrate[19,20] suggests that it might also deprotonate adduct **12** to afford intermediate I (Figure 6D). MD simulation studies performed on intermediate I revealed that most of the time W44 remains fixed between the side chain of Asp114 and Glu46, with one of its protons engaged in a hydrogen bond with a carboxylate oxygen of Asp114 and one of its oxygen's lone pairs pointing toward the external methylene group of the ligand (Figures 6A, S5, and S6). This water molecule is also in close contact with the guanidinium group of Arg48. In addition, the resulting dual-protonated His143 also continues to interact by hydrogen bonding with the C3 hydroxyl group of the ligand.

In this arrangement, the carboxylate group of Asp114 might be able to remove one of the protons of W44 to afford a hydroxide anion, which would be stabilized by the guanidinium group of Arg48. This hydroxide anion might then remove one of the hydrogen atoms of the methylene group of the ligand to trigger the dehydration of the C3 hydroxyl group, which would be assisted by His143 as a proton donor. A concerted mechanism might also be possible. As a result, enamine II, which is in equilibrium with its Schiff base **13**, would be obtained. The crystal structure of the latter adduct, which was

DOI: 10.1021/jacs.5b04080
J. Am. Chem. Soc. 2015, 137, 9333−9343

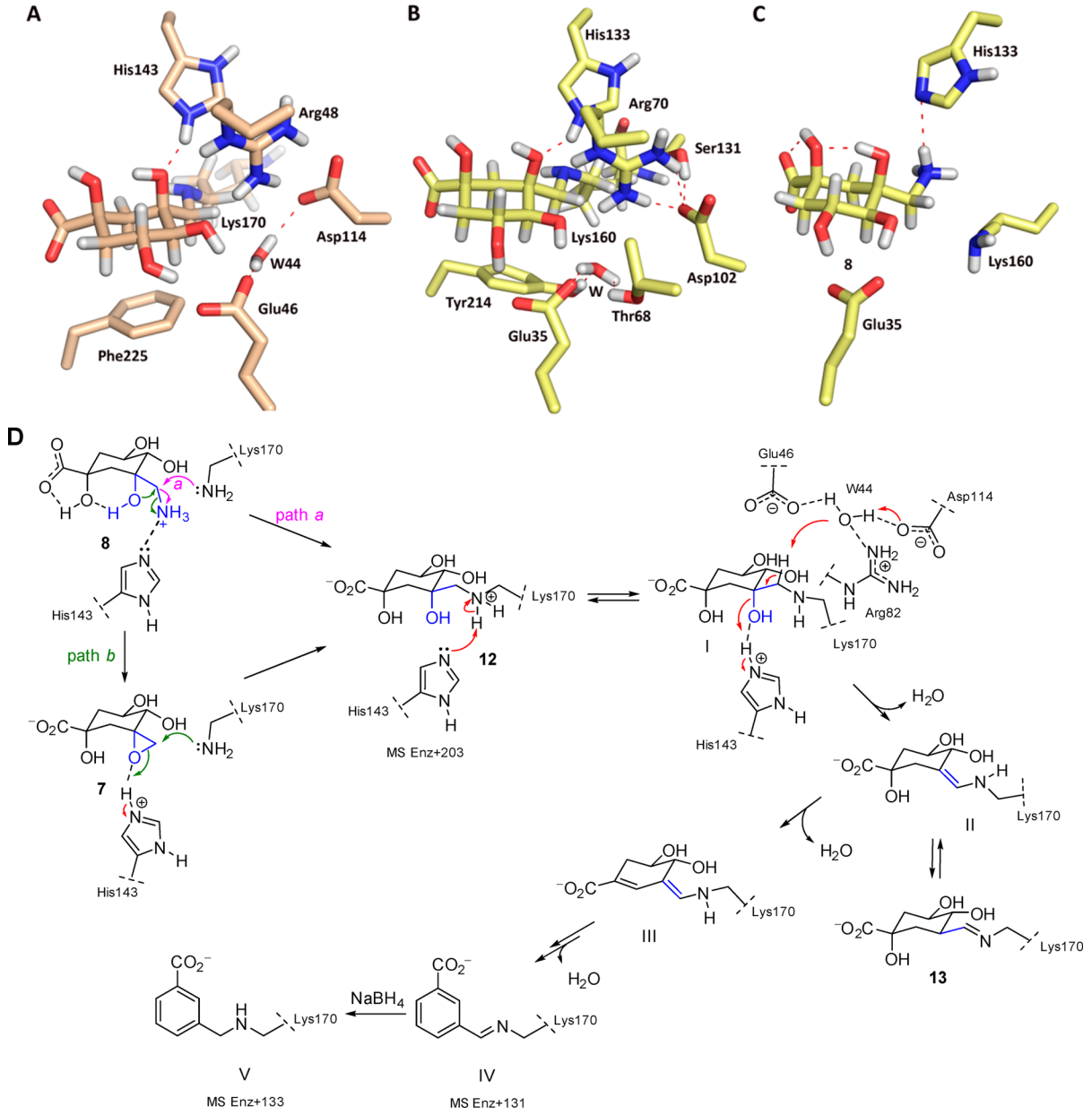

Figure 6. Proposed covalent modification mechanism (D) and representative snapshots of adduct I in *St*-DHQ1 (A) and *Sa*-DHQ1 (B) and plausible disposition of inhibitor **8** for covalent modification by an essential lysine (C, *Sa*-DHQ1) obtained by MD simulation studies. Relevant residues and the water molecule are indicated and labeled. Hydrogen bonds (red) are shown.

obtained by cocrystallization of *St*-DHQ1 with epoxide **7** after several weeks, has previously been solved.[17c] For *St*-DHQ1, the experimentally observed low mass peak (additional mass of 132) might be explained by aromatization of the resulting enamine II to give Schiff base IV (calculated mass increase of 131). The reduction of IV with sodium borohydride would afford amine/ammonium adduct V (calculated mass increase of 133).

For *Sa*-DHQ1, the mass spectrometry data indicate that a Schiff base is not formed. Instead, the enzyme is covalently modified by the formation of an amine. In an effort to explain these clear differences between the two enzymes, MD simulation studies were also performed with the *S. aureus* enzyme. The corresponding *Sa*-DHQ1/**8** adduct was modeled using the enzyme coordinates found in the crystal structure of the reduced form of the *Sa*-DHQ1 product-Schiff base intermediate (PDB entry 1SFJ)[8c] (see Experimental Section). Four possibilities were considered for *St*-DHQ1/**8**, i.e., a dual (δ and ε) and a single (δ) protonation state for His133 and free and protonated forms of Lys160 (Figure S7). In addition to the fact that the DHQ1 active site is highly conserved, comparison of the amino acid sequence in several DHQ1 enzymes revealed that Phe225 is replaced by a tyrosine (Tyr214) in *Sa*-DHQ1 (Figure S10). In contrast to *St*-DHQ1, in which the cyclohexane ring of the ligand is located on top of Phe225 by establishing key CH-π interactions with the axial hydrogens of the ring, in *Sa*-DHQ1 such interactions are only observed with the axial C2 hydrogen. The phenol ring of Tyr214 is shifted by around 2 Å toward the essential lysine binding pocket. In this arrangement, for intermediate I, the water molecule (W44 in *St*-DHQ1) interacts by hydrogen bonding with the phenolic group of Tyr124, the carboxylate group of the conserved Glu35,

DOI: 10.1021/jacs.5b04080
J. Am. Chem. Soc. 2015, 137, 9333−9343

and the side chain of Thr68 (Figures 6B, S8, and S9). More importantly, the carboxylate group of Asp102 (Asp114 in *S. typhi*) is located far away from this water molecule, and its position remains fixed by the guanidinium group of Arg70 (Arg48 in *S. typhi*) and the side chain of Ser131 throughout the whole simulation. Bearing in mind that (a) the carboxylate group of the conserved Glu35 (Glu46 in *S. typhi*) is mainly involved in a bidentate hydrogen bond with the C4 and C5 hydroxyl groups of the ligand and (b) the arrangement of this water molecule and Asp102 throughout the whole simulation, we considered that, for *Sa*-DHQ1, amino adduct I would be stable against dehydration, as observed experimentally. In contrast, the replacement of Tyr214 by Phe225 in *St*-DHQ1 causes changes in the position of the water molecule and its binding interactions that favor the elimination reaction (Figures S6 vs S9). These structural differences between the two enzymes might explain the differences obtained in the mass spectra. Moreover, computational studies on the binary complex DHQ1/**8**, initially modeled by molecular docking, using the program GOLD 5.2[21] followed by MD simulation studies suggest that, for both enzymes, the direct covalent linkage of the ammonium derivative **8** to the enzyme (Figure 6D, path a) would occur by nucleophilic attack of the lysine with the release of ammonia and by activation from the opposite site of the histidine acting as a Lewis acid (Figure 6C).

***In Vitro* Antivirulence Studies.** An experimental model of infection of A549 human alveolar epithelial cells was used to study the efficacy of compound **8** to inhibit the virulence of *Salmanella* Enteritidis. This was carried out by measuring the viability of A549 respiratory alveolar cells after infection using LIVE/DEAD staining. The mortality rates of alveolar cells incubated with the bacterial strain were determined and are showed in Figure 7. Co-incubation of the *Salmonella* Enteritidis clinical strain with the A549 cells resulted in a 37.1% decrease in A549 cell viability. Co-incubation of the A549 cells with the bacteria in the presence of 2 and 20 mg L^{-1} incremented the viability, showing 19.8% and 13.1% of cell death, respectively. Cells incubated only with compound **8** showed a similar viability than those not infected (<10% of deads cells), which reveals not toxic effects to the used concentrations. Thus, the addiction of ammonium derivative **8** to the medium reduced the ability of *Salmonella* Enteritidis to kill A549 respiratory cells compared to the control infection ($P < 0.05$).

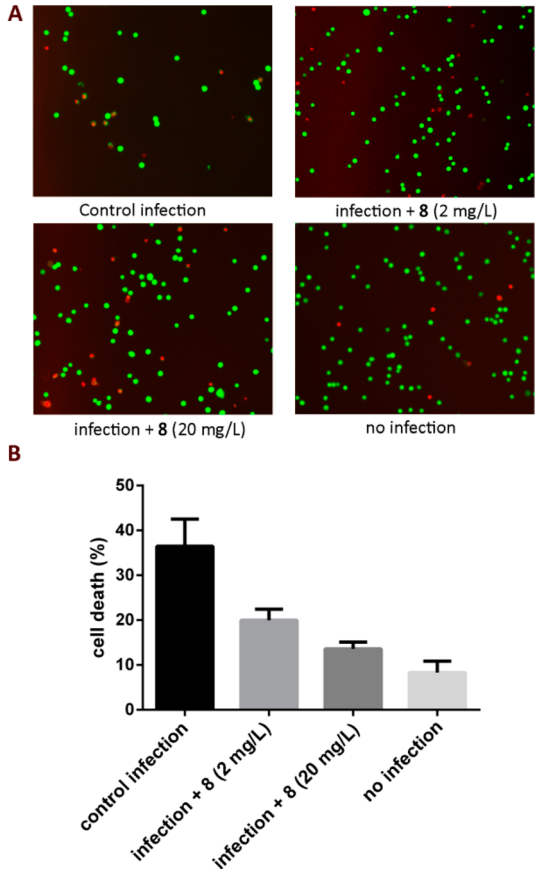

Figure 7. Efficacy of ammonium derivative **8** to inhibit the cell death of A549 alveolar cells by *Salmonella* Enteritidis infection. (A) Fluorescence microscopy images of human alveolar A549 cells infected with *Salmonella* Enteritidis clinical strain and stained with the LIVE/DEAD Cellstain double-staining kit. Stained green cells are healthy cells with intact membranes, and dead cells are stained red. A549 cells were incubated with *Salmonella* Enteritidis strain without compound **8** (1); with 2 mg L^{-1} of **8** (2); with 20 mg L^{-1} of **8** (3); and last, uninfected cells (4). (B) Quantification of A549 cell death caused by *Salmonella* Enteritidis. The results of four independent experiments are shown as means and SD. $P < 0.05$ between the treated and untreated cells.

CONCLUSIONS AND FINAL REMARKS

The first example of the chemical modification of the essential lysine active site of a dehydratase enzyme (DHQ1) by an ammonium derivative that does not bear reactive electrophilic centers is described. The irreversible inhibition of DHQ1 from *Salmonella typhi* and *Staphylococcus aureus*, which are involved in bacterial virulence, has been studied by a combination of biochemical, structural, and MD simulation studies. The resolution at 1.35 Å of the crystal structure of the *S. typhi* DHQ1 enzyme covalently modified by ammonium derivative **8**, which was obtained by soaking apo-*St*-DHQ1 crystals, revealed that the modified ligand is covalently attached to the essential Lys170 through the formation of an amine.

The results of inhibition studies and analysis by mass spectrometry of samples of inactivated enzymes showed clear differences between the two enzymes. The inactivation proved to be more efficient for *S. aureus* than for *S. typhi*. The results of this study provide strong evidence that the initial amine adduct of the *St*-DHQ1 enzyme undergoes further dehydration reactions involving Schiff base species, as evidenced by the mass spectra of samples treated with sodium borohydride. The covalent linkage between ammonium derivative **8** and DHQ1 would occur either by nucleophilic attack of the lysine with the release of ammonia and by activation from the opposite site of the histidine acting as a Lewis acid or via generation of the also irreversible inhibitor epoxide **7** by intramolecular cyclization of **8** in the DHQ1 active site and subsequent nucleophilic attack of the lysine. In the latter case, compound **8** would be a prodrug of epoxide **7**. Further experiments would be required to clarify this point.

The results of computational studies revealed that the replacement of Phe225 in *St*-DHQ1 by Tyr214 in *Sa*-DHQ1 and its hydrogen bonding interaction with the conserved water molecule, which has been observed in several crystal structures and is located in close contact to the NZ atom of the essential lysine, would prevent the initial amino adduct from undergoing dehydration/aromatization reactions. In contrast, for the *St*-DHQ1 enzyme this water molecule remains fixed between the side chain of the conserved Asp114 and Glu46 residues. In this arrangement, Asp114, with the assistance of the aforemen-

DOI: 10.1021/jacs.5b04080
J. Am. Chem. Soc. 2015, 137, 9333−9343

tioned water molecule, would be the base that triggers the dehydration of the C3 hydroxyl group with His143 acting as a proton donor. As a result, a Schiff base will be obtained that can undergo further dehydration reactions until full aromatization of the cyclohexane ring is achieved.

Antivirulence studies also showed that ammonium derivative **8** is able to reduce the ability of *Salmonella* Enteritidis to kill A549 respiratory cells *in vitro*.

The results presented here enhance our understanding of some of the determinants for the irreversible inhibition of this challenging multistep enzyme. These studies also show that the ammonium derivative **8** could be a good scaffold for the design of new inhibitors that can be used as drugs and opens up new opportunities for the development of novel antivirulence agents to combat widespread antibiotic resistance by targeting the DHQ1 enzyme.

EXPERIMENTAL SECTION

General. All starting materials and reagents were commercially available and were used without further purification. ^{1}H NMR spectra (250 and 500 MHz) and ^{13}C NMR spectra (63 and 125 MHz) were measured in deuterated solvents. *J* values are given in Hertz. NMR assignments were carried out by a combination of 1D, COSY, and DEPT-135 experiments. FT-IR spectra were recorded as NaCl plates or KBr discs. $[\alpha]_D^{20}$ = values are given in 10^{-1} deg cm^2 g^{-1}. Milli-Q deionized water was used in all the buffers. The spectroscopic measurements were made on a Varian Cary 100 UV−vis spectrophotometer with a 1 cm path length cell fitted with a Peltier temperature controller. Protein analysis was performed using an Ultraflex III TOF/TOF Bruker mass spectrometer.

*Methyl (1R,3S,4S,5R,6S,7S,9R)-7-azidomethyl-7,9-dihydroxy-3,4-dimethoxy-3,4-dimethyl-2,5-dioxabiciclo[4.4.0]decan-9-carboxylate (**10**).* A solution of epoxide **9**[17c] (479 mg, 1.44 mmol), sodium azide (1.12 g, 17.31 mmol), *p*-nitrobenzoic acid (240 mg, 1.44 mmol), and 15-crown-5 ether (290 μL, 1.45 mmol) in dry DMF (29 mL) and under inert atmosphere was heated at 115 °C for 1.5 h. After cooling to room temperature, the reaction mixture was diluted with ethyl acetate and water. The aqueous layer was separated, and the organic layer was washed with brine, dried (anh. Na_2SO_4), filtered, and concentrated under reduced pressure. Azide **10** (417 mg, 77%) was obtained as colorless oil. $[\alpha]_D^{20}$ = +114° (*c* 3.7, $CHCl_3$). ^{1}H NMR (250 MHz, $CDCl_3$) δ: 4.25 (m, 1H, H1), 3.79 (s, 3H, OCH_3), 3.67 (s, 1H, OH), 3.58 (d, *J* = 10.0 Hz, 1H, H6), 3.50 (d, *J* = 12.2 Hz, 1H, C*H*HN$_3$), 3.30 (d, *J* = 12.2 Hz, 1H, CH*H*N$_3$), 3.25 (s, 3H, OCH_3), 3.24 (s, 3H, OCH_3), 2.03 (m, 3H, CH_2−**10** + H8$_{eq}$), 1.91 (d, *J* = 12.2 Hz, 1H, H8$_{ax}$), 1.33 (s, 3H, CH_3) and 1.27 (s, 3H, CH_3) ppm. ^{13}C NMR (63 MHz, $CHCl_3$) δ: 174.4 (C), 100.3 (C), 99.5 (C), 74.9 (C), 74.4 (C), 72.0 (CH), 63.2 (CH), 55.8 (CH_2), 53.2 (OCH_3), 48.1 (OCH_3), 47.9 (OCH_3), 39.6 (CH_2), 38.2 (CH_2), 17.7 (CH_3) and 17.7 (CH_3) ppm. IR (KBr): υ 3458 (OH), 2104 (N≡N) and 1739 (CO) cm^{-1}. MS (ESI) *m*/*z* = 398 (MNa$^+$). HRMS calcd for $C_{15}H_{25}O_8N_3Na$ (MNa$^+$): 398.1534; found, 398.1537.

Hydrogenolysis of Azide 10. A suspension of azide **10** (406 mg, 1.08 mmol) and 10% palladium on carbon (70 mg) in methanol (30 mL) was stirred under hydrogen atmosphere at room temperature for 1.5 h. The mixture was filtered over Celite, and the residue was washed with methanol. The filtrate and washings were concentrated under reduced pressure. The obtained residue was disolved in dry DMF (11 mL) and treated with dry triethylamine (0.23 mL, 1.62 mmol) and di-*tert*-butyl dicarbonate (280 mg, 1.30 mmol). The mixture resulted was stirred at room temperature for 4 h and then diluted with ethyl acetate and water. The organic layer was separated, and the aqueous layer was extracted with ethyl acetate (× 3). All the organic extracts were dried (anh. Na_2SO_4), filtered, and concentrated under reduced pressure. The obtained residue was purified by flash chromatography on silica gel eluting with ethyl acetate/hexanes [1) (30:70); 2) (50:50)] to afford compound **11** (449 mg, 92%). $[\alpha]_D^{20}$ = +110° (*c* 2.8, $CHCl_3$). ^{1}H NMR (300 MHz, $CDCl_3$) δ: 4.95 (m, 1H, NH), 4.23 (m, 1H, H1), 3.76 (s, 3H, OCH_3), 3.50 (d, *J* = 9.9 Hz, 1H, H6), 3.46 (dd, *J* = 14.1 and 3.0 Hz, 1H, C*H*HNH), 3.24 (s, 3H, OCH_3), 3.22 (s, 3H, OCH_3), 3.19 (m, 1H, CH*H*NH), 2.07−1.87 (m, 3H, CH_2−**10** + H8$_{eq}$), 1.85 (d, *J* = 14.7 Hz, 1H, H8$_{ax}$), 1.41 (s, 9H, C(CH_3)$_3$), 1.32 (s, 3H, CH_3) and 1.26 (s, 3H, CH_3) ppm. ^{13}C NMR (75 MHz, $CDCl_3$) δ: 174.5 (C), 156.6 (C), 100.2 (C), 99.4 (C), 79.5 (C(CH_3)$_3$), 74.8 (C), 74.2 (C), 74.1 (CH), 63.4 (CH), 53.1 (OCH_3), 48.0 (OCH_3), 47.9 (OCH_3), 46.7 (CH_2), 39.4 (CH_2), 38.3 (CH_2), 28.3 (C(CH_3)$_3$) 17.7 (CH_3) and 17.7 (CH_3) ppm. IR (film): υ 3406 (OH + NH), 1739 (CO) and 1710 (CO) cm^{-1}. MS (ESI) *m*/*z* = 472 (MNa$^+$). HRMS calcd for $C_{20}H_{35}NO_{10}Na$ (MNa$^+$): 472.2153; found, 472.2137.

*(1R,3S,4S,5R)-1,3,4,5-Tetrahydroxy-3-methylamino-1-carboxylic acid (Hydrochloride Form) (**8**).* A solution of compound **11b** (28 mg, 0.05 mmol) in HCl (0.5 mL, 0.3 M) was heated at 100 °C for 1 h. After cooling to room temperature, the mixture was diluted with water and ethyl acetate. The organic layer was separated, and the aqueous layer was washed with ethyl acetate (× 2), and the aqueous extract was lyophilized to give amino acid **8** (12.5 mg, 97%) as a beige solid. $[\alpha]_D^{20}$ = −4° (*c* 1.7, CH_3OH). Mp: 148 °C (dec.). ^{1}H NMR (500 MHz, CD_3OD) δ: 3.98 (m, 1H, H5), 3.36 (d, *J* = 9.0 Hz, 1H, H4), 3.28 (d, *J* = 12.5 Hz, 1H, CH*H*NH$_3$), 2.89 (d, *J* = 12.5 Hz, 1H, CH*H*NH$_3$), 2.20 (ddd, *J* = 12.0, 4.0, and 2.0 Hz, 1H, H6$_{eq}$), 2.00 (d, *J* = 12.0 Hz, 1H, H2$_{ax}$), 1.97 (dd, *J* = 12.0 and 2.0 Hz, 1H, H2$_{eq}$) and 1.81 (dd, *J* = 12.0 and 13.0 Hz, 1H, H6$_{ax}$) ppm. ^{13}C NMR (125 MHz, CD_3OD) δ: 175.4 (C), 79.8 (CH), 76.4 (C), 73.3 (C), 68.4 (CH), 48.5 (CH_2), 42.2 (CH_2) and 40.1 (CH_2) ppm. IR (KBr): υ 3367 (OH + NH) and 1730 (CO) cm^{-1}. MS (ESI) *m*/*z* = 220 (M−H−HCl). HRMS calcd for $C_8H_{14}O_6$ (M−H−HCl): 220.0827; found, 220.0820.

Dehydroquinase Assays. The *St*-DHQ1 and *Sa*-DHQ1 enzymes were purified as described previously.[22,8c] Concentrated solutions of *St*-DHQ1 (0.85 mg mL^{-1}, 30.74 μM) and *Sa*-DHQ1 (4 mg mL^{-1}, 148.13 μM) were stored in potassium phosphate buffer (50 mM) and DTT (1 mM) at pH 6.6 and −80 °C. When required for assays, aliquots of the enzyme stocks were diluted in water and buffer and stored on ice. Dehydroquinase was assayed in the forward direction by monitoring the increase in absorbance at 234 nm in the UV spectrum due to the absorbance of the enone-carboxylate chromophore of 3-dehydroshikimic acid (**2**) (ε/M^{-1} cm^{-1} 12 000). Standard assay conditions were PPB (50 mM, pH 7.2) at 25 °C. Each assay was initiated by addition of the substrate. Solutions of 3-dehydroquinic acid (**1**) were calibrated by equilibration with DHQ1 and measurement of the change in the UV absorbance at 234 nm due to the formation of the enone-carboxylate chromophore of 3-dehydroshikimic acid (**2**). Under assay conditions, the kinetic parameters for *St*-DHQ1 and *Sa*-DHQ1 were K_m = 24 ± 3 μM; k_{cat} = 1.1 ± 0.1 s^{-1} and K_m = 18 ± 3 μM; k_{cat} = 255 ± 12 s^{-1}, respectively. Kinetic constants were evaluated using the GraFit 5 program (Erithacus Software Ltd.).

Inhibition Assays. Incubation of *St*-DHQ1 and *Sa*-DHQ1 (2.96 μM from a stock protein concentration of 0.85 mg mL^{-1} and 4 mg mL^{-1}, respectively) with various aqueous solutions of amino alcohol **8** (42−840 μM) was carried out in PPB (0.5 mL, 50 mM) at pH 7.2 and 5.8, 25 °C. The activity was progressively determined over a 24 h period under the standard assay conditions (see above) using aliquots from the incubation samples and the control.

Sodium Borohydride Inactivations. A 0.5 mL solution of *St*-DHQ1 (50 μL from a stock protein concentration of 0.85 mg mL^{-1}) in PPB (50 mM, pH 7.2) at 25 °C was incubated with compound **8** (200 μL from a stock concentration of 2.1 mM) for 1 h. After this incubation period, >90% reduction of the enzyme activity was observed. Under similar conditions, DHQ1 was also incubated with the natural substrate as a control. Several aliquots (10 μL) of a solution of sodium borohydride (20 mg mL^{-1}) in aqueous sodium hydroxide (40 mM) were then added. The DHQ1 activity was assayed before and after addition of sodium borohydride. After the sequential additions of aliquots of sodium borohydride solution (3 × 10 μL), full inactivation was observed for those control experiments carried out in the presence of the natural substrate. In the absence of the natural substrate or compound **8**, loss of activity was not observed after treatment with sodium borohydride. The samples were dialyzed using Amicon Ultra 0.5 centrifugal filters with 10 kDa cutoff by successive

DOI: 10.1021/jacs.5b04080
J. Am. Chem. Soc. 2015, 137, 9333−9343

addition of aqueous ammonium bicarbonate (× 4, 5 mM) and concentration. The samples were analyzed by mass spectrometry on a MALDI-TOF spectrometer with sinapinic acid as matrix.

Crystallization of the *St*-DHQ1/8 Adduct. Prism-shaped apo-*St*-DHQ1 crystals of up to 0.03 × 0.03 mm were obtained from a freshly purified solution of *St*-DHQ1 concentrated to 8 mg mL^{-1} in buffer A (10 mM Tris-HCl pH 7.4, 40 mM KCl) after 4 weeks of vapor diffusion in sitting drops comprised of 2.0 μL of protein solution mixed with 2.0 μL of reservoir solution and equilibrated against 0.15 mL reservoirs containing the crystallization mixture [25% (w/v) PEG 3350, 0.1 M Bis-Tris pH 5.5, 0.2 M magnesium chloride]. *St*-DHQ1/**8** adduct complex crystals were obtained after soaking during 24 h of apo-*St*-DHQ1 crystals in 10 mM solutions of ammonium derivative **8** in the crystallization mixture.

Structure Determination of the *St*-DHQ1/8 Adduct. Crystals were mounted into cryoloops and directly flash frozen by rapid immersion in liquid nitrogen. X-ray diffraction data were collected on beamline BM30A-FIP (ESRF, Grenoble, France) from a crystal maintained at 100 K. The diffraction data were processed, scaled, corrected for absorption effects, and the crystal unit-cell parameters were calculated by global refinement using XDS,[23] SCALA,[24] and other programs within the CCP4 software suite.[25] The structure was solved by molecular replacement, using the program MOLREP[26] with a search model generated from PDB entry 1QFE.[8c] The ligand structure and geometrical restraints were generated with the PRODRG2[27] server, and the structure was manually placed during the model building, which was performed with COOT.[28] Reflections used to calculate R_{free}[29] were selected randomly. The refinement of the models was performed with REFMAC,[30] and final structure validation was performed with MOLPROBITY.[31] The data collection, refinement, and model statistics are summarized in Table 1. Structure figures were prepared using PYMOL.[32]

Molecular Dynamics Simulations. *Ligand Preparation.* Lysine bound ligands were capped with the usual acetyl and methylamino groups. No bounded ligands were manually docked into the active site. Partial charges were derived by quantum mechanical calculations (HF/6-31G*) using Gaussian 09,[33] as implemented in the R.E.D. Server (version 3.0),[34] according to the RESP[35] model. The missing bonded and nonbonded parameters were assigned, by analogy or through interpolation from those already present in the AMBER database (GAFF).[36]

Generation and Minimization of the DHQ1-Ligand Adducts. (a) *St*-DHQ1 model: These studies were carried out using the enzyme coordinates found in the crystal structure of *St*-DHQ1/**8** adduct. (b) *Sa*-DHQ1 model: Simulations were carried out using the enzyme coordinates found in the crystal structure of the reduced form of the product-Schiff base intermediate of *Sa*-DHQ1 (PDB entry 1SFJ,[8c] chain A). Unsolved residues were added by superimposition with other chains and crystal structures (PDB entry 1SFL).[8c]

Crystallographic water molecules were maintained. Hydrogens were added, and protonation states to all titratable residues at the chosen pH of 7.0 were assigned using web-based H++ (version 3.1),[37] and WHAT-IF Optimal Hydrogen Bonding Network tool.[38] As a result of this analysis, for *Sa*-DHQ1 model, terminal groups of residues Asn25, Gln60, His132, Gln221, and Gln225 were rotated 180°. His3, His26, His114, and His166 were protonated in ε position, and His132 in δ position and His120 in both positions (δ and ε). For *St*-DHQ1 model, His51, His96, His146, His179, His194 were protonated in ε position and His132, His134 and His250 in both positions. Two protonation states for His143/His133 (δ or δ and ε) were considered as well as for the amino group of the ligand. Molecular mechanics parameters from the ff12SB[39] were assigned to the protein and the ligands using the LEaP module of AMBER 12.[40] Each molecular system was immersed in a truncated octahedron containing TIP3P[41] water molecules (10 Å radius) and Na+ ions[42] to achieve electroneutrality.

All systems were minimized in four stages: (a) initial minimization of the ligand (and the missing residues in *Sa*-DHQ1 model, residues 10−20 and 55−64) applying a restraint mask to the rest of the atoms; (b) minimization of the solvent and ions with a restraint mask to the protein and ligand; (c) minimization of the side chains, waters, and ions by applying a restraint mask to all α carbons; and (d) final minimization of the whole system. For all the cases a positional restraint force of 50 kcal mol^{-1} $Å^{-2}$ was used. 1000 steps were used for the first minimization and 5000 in the rest, with the first half of them using steepest descent method and the second half using conjugate gradient method.

Simulations. MD simulations were performed using the pmemd.-cuda_SPFP module[43] in AMBER 14[44] suite of programs and Amber ff12SB force field. Periodic boundary conditions were applied, and electrostatic interactions were treated using the smooth particle mesh Ewald method (PME)[45] with a grid spacing of 1 Å. The cutoff distance for the nonbonded interactions was 9 Å. The SHAKE algorithm[46] was applied to all bonds containing hydrogen, using a tolerance of 10^{-5} Å and an integration step of 2.0 fs. The minimized system was heated at 300 K (1 atm, 200 ps, a positional restraint force constant of 50 kcal mol^{-1} $Å^{-2}$ applied to all α carbons). Following equilibration under a constant volume (NVT) ensemble (200 ps, a positional restraint force constant of 5 kcal mol^{-1} $Å^{-2}$ applied to all α carbons); and six stages of equilibrations under a constant pressure (NPT) ensemble were carried out for 100 ps each, reducing gradually the initial force constraint from 5 to 0 kcal mol^{-1} $Å^{-2}$ in the final stage. MD simulations were carried out for 50 ns collecting system coordinates every 10 ps for further analysis.

***In Vitro* Antivirulence Studies.** An experimental model of infection of A549 human alveolar epithelial cells was used to study the efficacy of compound **8** to inhibit the virulence of *Salmonella* Enteritidis. Cells were cultured in Dulbecco modified Eagle medium (DMEM) supplemented with 10% fetal bovine serum, 100 mg L^{-1} of penicillin, and 100 mg L^{-1} streptomycin at 37 °C in the presence of 10% CO_2. For cell viability assays, monolayers of A549 cells were cultured in 24-well plates to a density of 10^5 cells per well. Later, the cells were infected with 15×10^7 colony-forming units (CFU) per well of a clinical strain of *Salmonella* Enteritidis isolated in the A Coruña Hospital. New DMEM with 2 or 20 mg L^{-1} of compound **8** was added to the cells and was grown for 4 h at 37 °C. Controls without the bacterial infection and without inhibitor **8** were used. The number of inoculated bacteria was determined by direct plating. A LIVE/DEAD fluorescence microscopy kit (Cellstain double-staining kit; Fluka, Buchs, Switzerland) was used according to the manufacturer's instructions to measure cell viability postinfection. The A549 cells were incubated for 15 min at 37 °C with phosphate-buffered saline (PBS) containing a mixture of the two fluorescent molecules to obtain simultaneous fluorescent staining; calcein-AM is able to stain viable cells (green), while propidium iodide can stain only dead cells (red). Microscopic images of the stained cells (alive and dead) were obtained using an inverted fluorescence microscope (Nikon Eclipse Ti) and analyzed with the NIS Elements Br software package.[47] At least four replicates of each assay were analyzed, and the statistical significance was determined using Student's *t* test.

■ ASSOCIATED CONTENT

Ⓢ Supporting Information

Coordinates and structure factors are available from the Protein Data Bank with accession code 4UIO. Extra figures for the structural and computational studies are included. The Supporting Information is available free of charge on the ACS Publications website at DOI: 10.1021/jacs.5b04080.

■ AUTHOR INFORMATION

Corresponding Author

*concepcion.gonzalez.bello@usc.es

Notes

The authors declare no competing financial interest.

■ ACKNOWLEDGMENTS

Financial support from the Spanish Ministry of Science and Innovation (SAF2013-42899-R), Xunta de Galicia (GRC2013-

DOI: 10.1021/jacs.5b04080
J. Am. Chem. Soc. 2015, 137, 9333−9343

041), and the European Regional Development Fund (ERDF) is gratefully acknowledged. E.L. thanks the Xunta de Galicia for his postdoctoral fellowship. A.B. thanks the Miguel Servet Programme ISCIII-FEDER (CP13/00226) and the ISCIII-General Subdirection of Assesment and Promotion of the Research (PI14/00059) for financial support. We are grateful to the ESRF synchrotron (Grenoble, France) for the provision of beam time and to the Centro de Supercomputación de Galicia (CESGA) for use of the Finis Terrae computer. We also thank Dr. F. J. Cañada for hepful disscussions.

REFERENCES

(1) Coates, A.; Hu, Y.; Bax, R.; Page, C. *Nat. Rev. Drug Discovery* **2002**, *1*, 895−910.
(2) Clatworthy, A. E.; Pierson, E.; Hung, D. T. *Nat. Chem. Biol.* **2007**, *3*, 541−548.
(3) (a) Payne, D. J.; Gwynn, M. N.; Holmes, D. J.; Pompliano, D. L. *Nat. Rev. Drug Discovery* **2007**, *6*, 29−40. (b) Walsh, C. *Nature* **2000**, *406*, 775−781. (c) Projan, S. J. *Curr. Opin. Pharmacol.* **2002**, *2*, 513−544.
(4) (a) Allen, R. C.; Popat, R.; Diggle, S. P.; Brown, S. P. *Nat. Rev. Microbiol.* **2014**, *12*, 300−308. (b) Cegelski, L.; Marshall, G. R.; Eldridge, G. R.; Hultgren, S. J. *Nat. Rev. Microbiol.* **2008**, *6*, 17−27. (c) ÓConnell, K. M. G.; Hodgkinson, J. T.; Sore, H. F.; Welch, M.; Salmond, G. P. C.; Spring, D. R. *Angew. Chem., Int. Ed.* **2013**, *52*, 10706−10733.
(5) (a) Tacket, C. O.; Hone, D. M.; Curtiss, R., III; Kelly, S. M.; Losonsky, G.; Guers, L.; Harris, A. M.; Edelman, R.; Levine, M. M. *Infect. Immun.* **1992**, *60*, 536−541. (b) Karnell, A.; Cam, P. D.; Verma, N.; Lindberg, A. A. *Vaccine* **1993**, *11*, 830−836. (c) Tacket, C. O.; Hone, D. M.; Losonsky, G.; Guers, L.; Edelman, R.; Levine, M. M. *Vaccine* **1992**, *10*, 443−446. (d) Racz, R.; Chung, M.; Xiang, Z.; He, Y. *Vaccine* **2013**, *31*, 797−805.
(6) (a) Chauduri, C.; Ducan, K.; Graham, L. D.; Coggins, J. R. *Biochem. J.* **1991**, *275*, 1−6. (b) Shneier, A.; Kleanthous, C.; Deka, R.; Coggins, J. R.; Abell, C. *J. Am. Chem. Soc.* **1991**, *113*, 9416−9418. (c) Harris, J.; Kleanthous, C.; Coggins, J. R.; Hawkins, A. R.; Abell, C. *J. Chem. Soc., Chem. Commun.* **1993**, 1080−1081. (d) Leech, A. P.; James, R.; Coggins, J. R.; Kleanthous, C. *J. Biol. Chem.* **1995**, *270*, 25827−25836. (e) Smith, B. W.; Turner, M. J.; Haslam, E. *J. Chem. Soc., Perkin Trans. 1* **1975**, 52−53. (f) Vaz, A. D. N.; Butler, J. R.; Nugent, M. J. *J. Am. Chem. Soc.* **1975**, *97*, 5914−5920.
(7) Light, S. H.; Minasov, G.; Shuvalova, L.; Duban, M. E.; Caffrey, M.; Anderson, W. F.; Lavie, A. *J. Biol. Chem.* **2011**, *286*, 3531−3539.
(8) (a) Krell, T.; Horsbourgh, M. J.; Cooper, A.; Kelly, S. M.; Coggins, J. R. *J. Biol. Chem.* **1996**, *271*, 24492−24497. (b) Deka, R. K.; Kleanthous, C.; Coggins, J. R. *J. Biol. Chem.* **1992**, *267*, 22237−22242. (c) Nichols, C. E.; Lockyer, M.; Hawkins, A. R.; Stammers, D. K. *Proteins: Struct., Funct., Genet.* **2004**, *56*, 625−628.
(9) Kleanthous, C. K.; Deka, R.; Davis, K.; Kelly, S. M.; Cooper, A.; Harding, S. E.; Price, N. C.; Hawkins, A. R.; Coggins, J. R. *Biochem. J.* **1992**, *282*, 687−695.
(10) Gourley, D. G.; Shrive, A. K.; Polikarpov, I.; Krell, T.; Coggins, J. R.; Hawkins, A. R.; Isaacs, N. W.; Sawyer, L. *Nat. Struct. Biol.* **1999**, *6*, 521−525.
(11) (a) Harris, J.; González-Bello, C.; Kleanthous, C.; Coggins, J. R.; Hawkins, A. R.; Abell, C. *Biochem. J.* **1996**, *319*, 333−336. (b) Coderch, C.; Lence, E.; Peón, A.; Lamb, H.; Hawkins, A. R.; Gago, F.; González-Bello, C. *Biochem. J.* **2014**, *458*, 547−557. (c) González-Bello, C. *Curr. Top. Med. Chem.* **2015**, accepted.
(12) Lamichhane, G.; Freundlich, J. S.; Ekins, S.; Wickramaratne, N.; Nolan, S. T.; Bisha, W. R. *mBio* **2011**, *2*, e00301−10.
(13) (a) Lence, L.; Tizón, L.; Otero, J. M.; Peón, A.; Prazeres, V. F. V.; Llamas-Saiz, A. L.; Fox, G. C.; van Raaij, M. J.; Lamb, H.; Hawkins, A. R.; González-Bello, C. *ACS Chem. Biol.* **2013**, *8*, 568−577. (b) Peón, A.; Otero, J. M.; Tizón, L.; Prazeres, V. F. V.; Llamas-Saiz, A. L.; Fox, G. C.; van Raaij, M. J.; Lamb, H.; Hawkins, A. R.; Gago, F.; Castedo, L.; González-Bello, C. *ChemMedChem* **2010**, *5*, 1726−1733.
(14) (a) Prazeres, V. F. V.; Sánchez-Sixto, C.; Castedo, L.; Lamb, H.; Hawkins, A. R.; Riboldi-Tunnicliffe, A.; Coggins, J. R.; Lapthorn, A. J.; González-Bello, C. *ChemMedChem* **2007**, *2*, 194−207. (b) Toscano, M. D.; Payne, R. J.; Chiba, A.; Kerbarh, O.; Abell, C. *ChemMedChem* **2007**, *2*, 101−112. (c) Payne, R. J.; Riboldi-Tunnicliffe, A.; Kerbarh, O.; Abell, A. D.; Lapthorn, A. J.; Abell, C. *ChemMedChem* **2007**, *2*, 1010−1013. (d) Payne, R. J.; Peyrot, F.; Kerbarh, O.; Abell, A. D.; Abell, C. *ChemMedChem* **2007**, *2*, 1015−1029. (e) Sánchez-Sixto, C.; Prazeres, V. F. V.; Castedo, L.; Shuh, S. W.; Lamb, H.; Hawkins, A. R.; Cañada, F. J.; Jiménez-Barbero, J.; González-Bello, C. *ChemMedChem* **2008**, *3*, 756−770. (f) Tran, A. T.; Cergol, K. M.; Britton, W. J.; Bokhari, S. A. I.; Ibrahim, M.; Lapthorn, A. J.; Payne, R. J. *MedChemComm* **2010**, *1*, 271−275. (g) Prazeres, V. F. V.; Tizón, L.; Otero, J. M.; Guardado-Calvo, P.; Llamas-Saiz, A. L.; van Raaij, M. J.; Castedo, L.; Lamb, H.; Hawkins, A. R.; González-Bello, C. *J. Med. Chem.* **2010**, *53*, 191−200. (h) Tran, A. T.; Cergol, K. M.; West, N. P.; Randall, E. J.; Britton, W. J.; Bokhari, S. A.; Ibrahim, M.; Lapthorn, A. J.; Payne, R. J. *ChemMedChem* **2011**, *6*, 262−265. (i) Paz, S.; Tizón, L.; Otero, J. M.; Llamas-Saiz, A. L.; Fox, G. C.; van Raaij, M. J.; Lamb, H.; Hawkins, A. R.; Lapthorn, A. J.; Castedo, L.; González-Bello, C. *ChemMedChem* **2011**, *6*, 266−272. (j) Dias, M. V. B.; Snee, W. C.; Bromfield, K. M.; Payne, R. J.; Palaninathan, S. K.; Ciulli, A.; Howard, N. I.; Abell, C.; Sacchettini, J. C.; Blundell, T. L. *Biochem. J.* **2011**, *436*, 729−739. (k) Blanco, B.; Sedes, A.; Peón, A.; Lamb, H.; Hawkins, A. R.; Castedo, L.; González-Bello, C. *Org. Biomol. Chem.* **2012**, *10*, 3662−3676. (l) Blanco, B.; Sedes, A.; Peón, A.; Otero, J. M.; van Raaij, M. J.; Thompson, P.; Hawkins, A. R.; González-Bello, C. *J. Med. Chem.* **2014**, *57*, 3494−3510. (m) Peón, A.; Coderch, C.; Gago, F.; González-Bello, C. *ChemMedChem* **2013**, *8*, 740−747.
(15) Tizón, L.; Otero, J. M.; Prazeres, V. F. V.; Llamas-Saiz, A. L.; Fox, G. C.; van Raaij, M. J.; Lamb, H.; Hawkins, A. R.; Ainsa, J. A.; Castedo, L.; González-Bello, C. *J. Med. Chem.* **2011**, *54*, 6063−6084.
(16) Howard, N. I.; Dias, M. V. B.; Peyrot, F.; Chen, L.; Schmidt, M. F.; Blundell, T. L.; Abell, C. *ChemMedChem* **2015**, *10*, 116−133.
(17) (a) Bugg, T. D. H.; Abell, C.; Coggins, J. R. *Tetrahedron Lett.* **1988**, *29*, 6783−6786. (b) González-Bello, C.; Harris, J. M.; Manthey, M. K.; Coggins, J. R.; Abell, C. *Bioorg. Med. Chem. Lett.* **2000**, *10*, 407−409. (c) Tizón, L.; Maneiro, M.; Peón, A.; Otero, J. M.; Lence, E.; Poza, S.; van Raaij, M. J.; Thompson, P.; Hawkins, A. R.; González-Bello, C. *Org. Biomol. Chem.* **2015**, *13*, 706−716.
(18) For non-covalent DHQ1 inhibitors see: Ratia, K.; Light, S. H.; Antanasijevic, A.; Anderson, W. F.; Caffrey, M.; Lavie, A. *PLoS One* **2014**, *9*, e89356−e89363.
(19) Yao, Y.; Li, Z.-S. *Chem. Phys. Lett.* **2012**, *519*−*520*, 100−104.
(20) Maneiro, M.; Peón, A.; Lence, E.; Otero, J. M.; van Raaij, M. J.; Thompson, P.; Hawkins, A. R.; González-Bello, C. *Biochem. J.* **2014**, *462*, 415−424.
(21) *Cambridge Crystallographic Data Center*; http://www.ccdc.cam.ac.uk/products/life_sciencies/gold/ (accessed Feb 2, 2015).
(22) Moore, J. D.; Hawkins, A. R.; Charles, I. G.; Deka, R.; Coggins, J. R.; Cooper, A.; Kelly, S: M.; Price, N. C. *Biochem. J.* **1993**, *295*, 277−285.
(23) Kabsch, W. *Acta Crystallogr., Sect. D: Biol. Crystallogr.* **2010**, *66*, 125−132.
(24) Evans, P. *Acta Crystallogr., Sect. D: Biol. Crystallogr.* **2006**, *62*, 72−82.
(25) Winn, M. D. *J. Synchrotron Radiat.* **2003**, *10*, 23−25.
(26) Vagin, A.; Teplyakov, A. *J. Appl. Crystallogr.* **1997**, *30*, 1022−1025.
(27) Schüttelkopf, A. W.; van Aalten, D. M. F. *Acta Crystallogr., Sect. D: Biol. Crystallogr.* **2004**, *60*, 1355−1363.
(28) Emsley, P.; Cowtan, K. *Acta Crystallogr., Sect. D: Biol. Crystallogr.* **2004**, *60*, 2126−2132.
(29) Brünger, A. T. *Methods Enzymol.* **1997**, *277*, 366−396.
(30) Murshudov, G. N.; Vagin, A. A.; Dodson, E. J. *Acta Crystallogr., Sect. D: Biol. Crystallogr.* **1997**, *53*, 240−255.
(31) Davis, I. W.; Leaver-Fay, A.; Chen, V. B.; Block, J. N.; Kapral, G. J.; Wang, X.; Murray, L. W.; Arendall, W. B., 3rd; Snoeyink, J.;

DOI: 10.1021/jacs.5b04080
J. Am. Chem. Soc. 2015, 137, 9333−9343

Richardson, J. S.; Richardson, D. C. *Nucleic Acids Res.* **2007**, *35*, W375−W383.
(32) DeLano, W. L. *The PyMOL Molecular Graphics System*; DeLano Scientific LLC: Palo Alto, CA, 2008. http://www.pymol.org/.
(33) Frisch, M. J.; Trucks, G. W.; Schlegel, H. B.; Scuseria, G. E.; Robb, M. A.; Cheeseman, J. R.; Scalmani, G.; Barone, V.; Mennucci, B.; Petersson, G. A.; Nakatsuji, H.; Caricato, M.; Li, X.; Hratchian, H. P.; Izmaylov, A. F.; Bloino, J.; Zheng, G.; Sonnenberg, J. L.; Hada, M.; Ehara, M.; Toyota, K.; Fukuda, R.; Hasegawa, J.; Ishida, M.; Nakajima, T.; Honda, Y.; Kitao, O.; Nakai, H.; Vreven, T.; Montgomery, J. A., Jr.; Peralta, J. E.; Ogliaro, F.; Bearpark, M.; Heyd, J. J.; Brothers, E.; Kudin, K. N.; Staroverov, V. N.; Kobayashi, R.; Normand, J.; Raghavachari, K.; Rendell, A.; Burant, J. C.; Iyengar, S. S.; Tomasi, J.; Cossi, M.; Rega, N.; Millam, J. M.; Klene, M.; Knox, J. E.; Cross, J. B.; Bakken, V.; Adamo, C.; Jaramillo, J.; Gomperts, R.; Stratmann, R. E.; Yazyev, O.; Austin, A. J.; Cammi, R.; Pomelli, C.; Ochterski, J. W.; Martin, R. L.; Morokuma, K.; Zakrzewski, V. G.; Voth, G. A.; Salvador, P.; Dannenberg, J. J.; Dapprich, S.; Daniels, A. D.; Farkas, Ö.; Foresman, J. B.; Ortiz, J. V.; Cioslowski, J.; Fox, D. J. *Gaussian 09*, Revision D.01; Gaussian, Inc.: Wallingford, CT, 2009.
(34) (a) Vanquelef, E.; Simon, S.; Marquant, G.; Garcia, E.; Klimerak, G.; Delepine, J. C.; Cieplak, P.; Dupradeau, F.-Y. *Nucleic Acids Res.* **2011**, *39*, W511−W517. (b) Dupradeau, F.-Y.; Pigache, A.; Zaffran, T.; Savineau, C.; Lelong, R.; Grivel, N.; Lelong, D.; Rosanski, W.; Cieplak, P. *Phys. Chem. Chem. Phys.* **2010**, *12*, 7821−7839.
(35) Bayly, C. I.; Cieplak, P.; Cornell, W.; Kollman, P. A. *J. Phys. Chem.* **1993**, *97*, 10269−10280.
(36) Wang, J.; Wang, W.; Kollman, P. A.; Case, D. A. *J. Mol. Graphics Modell.* **2006**, *25*, 247−260.
(37) Anandakrishnan, R.; Aguilar, B.; Onufriev, A. V. *Nucleic Acids Res.* **2012**, *40*, W537−W541.
(38) Hooft, R. W. W.; Sander, C.; Vriend, G. *Proteins: Struct., Funct., Genet.* **1996**, *26*, 363−376.
(39) Hornak, V.; Abel, R.; Okur, A.; Strockbine, B.; Roitberg, A.; Simmerling, C. *Proteins: Struct., Funct., Genet.* **2006**, *65*, 712−725.
(40) Case, D. A.; Darden, T. A.; Cheatham, T. E., III; Simmerling, C. L.; Wang, J.; Duke, R. E.; Luo, R.; Walker, R. C.; Zhang, W.; Merz, K. M.; Roberts, B.; Hayik, S.; Roitberg, A.; Seabra, G.; Swails, J.; Goetz, A. W.; Kolossváry, I.; Wong, K. F.; Paesani, F.; Vanicek, J.; Wolf, R. M.; Liu, J.; Wu, X.; Brozell, S. R.; Steinbrecher, T.; Gohlke, H.; Cai, Q.; Ye, X.; Wang, J.; Hsieh, M.-J.; Cui, G.; Roe, D. R.; Mathews, D. H.; Seetin, M. G.; Salomon-Ferrer, R.; Sagui, C.; Babin, V.; Luchko, T.; Gusarov, S.; Kovalenko, A.; Kollman, P. A. *Amber Tools 13 and Amber 12*; University of California: San Francisco, CA, 2012.
(41) Jorgensen, W. L.; Chandrasekhar, J.; Madura, J. D. *J. Chem. Phys.* **1983**, *79*, 926−935.
(42) Joung, S.; Cheatham, T. E. *J. Phys. Chem. B* **2008**, *112*, 9020−9041.
(43) Le Grand, S.; Goetz, A. W.; Walker, R. C. *Comput. Phys. Commun.* **2013**, *184*, 374−380.
(44) Case, D. A.; Babin, V.; Berryman, J. T.; Betz, R. M.; Cai, Q.; Cerutti, D. S.; Cheatham, T. E., III; Darden, T. A.; Duke, R. E.; Gohlke, H.; Goetz, A. W.; Gusarov, S.; Homeyer, N.; Janowski, P.; Kaus, J.; Kolossváry, I.; Kovalenko, A.; Lee, T. S.; Le Grand, S.; Luchko, T.; Luo, R.; Madej, B.; Merz, K. M.; Paesani, F.; Roe, D. R.; Roitberg, A.; Sagui, C.; Salomon-Ferrer, R.; Seabra, G.; Simmerling, C. L.; Smith, W.; Swails, J.; Walker, R. C.; Wang, J.; Wolf, R. M., Wu, X.; Kollman, P. A. *AMBER 14*; University of California: San Francisco, CA, 2014.
(45) Salomon-Ferrer, R.; Goetz, A. W.; Poole, D.; Le Grand, S.; Walker, R. C. *J. Chem. Theory Comput.* **2013**, *9*, 3878−3888.
(46) Ryckaert, J.-P.; Ciccotti, G.; Berendsen, H. J. C. *J. Comput. Phys.* **1977**, *23*, 327−341.
(47) Beceiro, A.; Moreno, A.; Fernández, N.; Vallejo, J. A.; Aranda, J.; Adler, B.; Harper, M.; Boyce, J. D.; Bou, G. *Antimicrob. Agents Chemother.* **2014**, *58*, 518−526.

DOI: 10.1021/jacs.5b04080
J. Am. Chem. Soc. 2015, 137, 9333−9343